Comparative study of the I-V scaling in highly anisotropic $Bi_2Sr_2CaCu_2O_{8+\delta}$ and isotropic $(K,Ba)BiO_3$ heavy-ion-irradiated single crystals

L. Ammor,* B. Pignon, and A. Ruyter
Laboratoire d'Electrodynamique des Matériaux Avancés, UMR 6157 CNRS-CEA, Université F. Rabelais, UFR Sciences, Parc de Grandmont, 37200 Tours, France

(Received 25 November 2003; published 19 April 2004; corrected 24 May 2004)

The Bose-glass transition has been investigated by transport measurements on heavy-ion irradiated $Bi_2Sr_2CaCu_2O_{8+\delta}$ and isotropic $(K,Ba)BiO_3$ single crystals. When a magnetic field was applied parallel to the defects, we show that, for $B_\phi/10<\mu_0 H<B_\phi$, the same scaling functions could be used to describe the transition in these two systems emphasizing the universality of this transition. The field and sample-independent critical exponents which were found to be $\nu_\perp=1.1\pm0.1$, $z=5.3\pm0.2$, and $\alpha(\equiv\nu_\parallel/\nu_\perp)=2$, are consistent with Monte Carlo simulations with screened vortex interactions and columnar defects. In addition, we found that in both systems, the creep process in the Bose glass phase could be described by the variable-range hopping mechanism of flux lines with the glassy exponent value of $\mu=1/3$ which is close to the transition and the creep exponent $\mu\approx1$ at lower temperatures suggests that creep is then dominated by a generation of half loops expanding along the track direction.

DOI: 10.1103/PhysRevB.69.134508 PACS number(s): 74.25.Fy, 74.72.Hs, 74.25.Qt

I. INTRODUCTION

It is now well established that the random distributed parallel columnar defects (CDs) produced by heavy-ion irradiation in high-T_c superconductors (HTSs) lead to formation of a so-called Bose-glass phase, where vortices are localized at the columnar defects.[1] It is predicted that this phase melts into an entangled liquid through a second-order transition at high temperature. The ''strongly'' Bose glass is only expected to exist below the accommodation field $(\mu_0 H)^* \sim B_\phi/3-B_\phi$ depending on the system and the irradiation dose (where B_ϕ is the matching, on average, each columnar defect is occupied by one vortex). For higher magnetic fields, interstitial vortices lead to a formation of a ''weakly'' pinned Bose glass phase, which cannot be described by the critical scaling behavior.[2] One signature of a Bose-glass-to-vortex liquid transition is the universal scaling of current-voltage characteristics with well-defined critical exponents. This has been verified in several experiments[3–6] and in numerical simulations,[7] both in highly anisotropic $Bi_2Sr_2CaCu_2O_{8+\delta}$ (BSCCO) and weakly anisotropic $YBa_2Cu_3O_{7-\delta}$ (YBCO) compounds. The main difference between these two systems is their anisotropy factor as $\gamma=(m_c/m_{ab})^{1/2}>1$, where m_c and m_{ab} denote the effective masses of electrons moving along the c axis and the ab plane, respectively. Numerous studies performed in these materials indicated that the value of the electronic anisotropy strongly affects the static and dynamic properties of the vortex matter in the presence of CDs.[8,9] For example, the three-dimensional Bose glass was observed at fields below the matching field B_ϕ by ac magnetic susceptibility measurements in irradiated BSCCO:2212 ($\gamma\sim50-100$), while it was not observed in irradiated $Bi_2(Sr,La)_2CuO_{6+\delta}$ (Bi-2201).[9] This difference is due to the extremely weak coupling between pancake vortices along the c axis in Bi-2201 ($\gamma=700$) even under the presence of columnar defects. It is interesting to investigate the anisotropy effect on the critical scaling of current-voltage characteristics near the Bose-glass transition, and this is the subject of this paper.

In this work, we present a comparative study of the vortex dynamics between the highly anisotropic BSCCO and the fully isotropic $(K,Ba)BiO_3$ (KBBO) systems with columnar defects. The KBBO superconductor ($T_c\sim30$ K) appears to be particularly interesting since it present a fully isotropic cubic structure and a phase diagram, which is experimentally accessible down to the lowest temperature. In addition, transport and neutron diffraction measurements on the vortex lattice in this system yield the results, which are very similar to the phenomenology of HTSs.[10,11] The paper is organized as follows: We begin by describing the sample preparation and experiments. We divide Sec. III into two parts. In Sec. III A, the universality of the critical behavior of the resistivity around T_{BG} is explored using I-V measurements. We show that, for magnetic fields $B_\phi/10<\mu_0 H<B_\phi$, the same scaling functions with a single set of critical exponents [$\nu_\perp=1.1\pm0.1$, $z=5.3\pm0.2$ and $\alpha(\equiv\nu_\parallel/\nu_\perp)=2$] can be used to rescale the I-V characteristics of both BSCCO and KBBO systems emphasizing the universality of the transition in this field range. Finally, the Sec. III B is focused on the creep mechanisms in the Bose glass phase in both systems. A quantitative analysis of $V(I)$ curves indicates that the vortex creep is dominated by the nucleation of vortex kinks as half-loops and tunnelling between different columnar defects via the formation of a pair of ''superkinks.''

II. SAMPLE PREPARATION AND EXPERIMENT

Experiments were performed on three BSCCO and two $(K,Ba)BiO_3$ single crystals. Three BSCCO single crystals were used in this study: $Bi_{1.8}Pb_{0.2}Sr_2CaCu_2O_{8+\delta}$ (sample 1, $T_c=80.0$ K), BSCCO (sample 2, $T_c=89.5$ K) and $Bi_2Sr_2Ca_{0.64}Y_{0.36}Cu_2O_{8+\delta}$ (sample 3, $T_c=91.2$ K). All of them were grown by a self flux method which was described elsewhere.[12] The anisotropy parameter, $\gamma\sim50-100$, was estimated by resistivity measurements on the unirradiated ref-

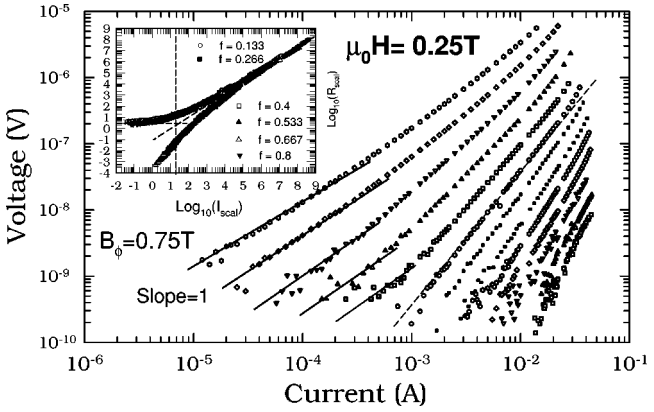

FIG. 1. Typical I-V characteristics around T_{BG} for the sample 1 at $\mu_0 H = 0.25$ T. From the right to the left, the data were obtained at the following temperatures: 59.38, 59.95, 60.52, 61.09, 61.67, 62.23, 62.81, 63.38, 63.96, 64.53, 65.11, 65.68, and 66.25 K. The solid lines indicate the linear response observed at high temperatures for low currents. The inset shows the scaling collapse with the ordinate $R_{\mathrm{scal}} = (V/I)/|t|^{\nu_\perp(z-2)}$ and the abscissa $I_{\mathrm{scal}} = I/(T|t|^{3\nu_\perp})$, at indicated filling fractions f according to Eq. (1).

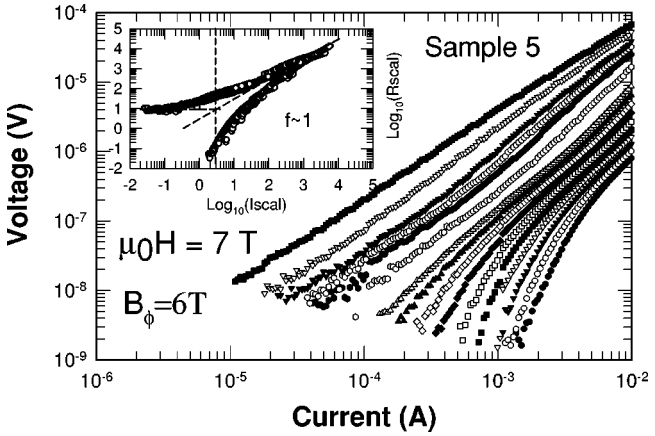

FIG. 2. Current voltage characteristics of the irradiated KBBO crystal (sample 5, $B_\phi = 6$ T) taken at $\mu_0 H = 7\ \mathrm{T} \sim B_\phi$. Temperature range is 19.0–20.5 K with a step of 0.1 K. The inset denotes the scaling collapse of the same data.

erence samples. The samples with a typical dimension of $0.4 \times 1 \times 0.02\ \mathrm{mm}^3$ were irradiated with a beam of 6-GeV Pb ions (which traversed over the entire specimen) at the Grand Accelerateur National d'Ions Lourds (GANIL, Caen-France). Parallel columnar defects of a radius $c_0 \sim 40$ Å, throughout the thickness of the samples, were created along the c axis with a matching dose of $B_\phi = 0.75$ T for samples 1 and 3 and $B_\phi = 1.5$ T for sample 2.[13] Here, the matching field B_ϕ is defined as $B_\phi = n_d \phi_0$, where n_d is the density of the columnar defects and ϕ_0 is the flux quantum.

The (K,Ba)BiO_3 single crystals were grown by the electrocrystalization and $w \sim 100$ μm thick slices were irradiated with 7.2-GeV Ta ions. The experiments were performed on two samples with $B_\phi = 1$ T (sample 4, $T_c \sim 28.0$ K) and $B_\phi = 6$ T (sample 5, $T_c \sim 31.5$ K). As pointed out in Ref. 14, transmission electron micrographs showed that the irradiation results in the formation of linear amorphous tracks of a radius $c_0 \sim 30-40$ Å and produces only a very small change in zero field transition temperature. I-V characteristics were obtained by using a standard dc four-probe method with a voltage resolution of 0.5 nV and a temperature stability better than 5 mK. The magnetic field was aligned with the ions tracks using a well-known dip feature occurring in dissipation for the fields parallel to the columnar defects.

III. RESULTS AND DISCUSSIONS

A. Scaling analysis of current-voltage characteristics

We examined the shape of the I-V curves in the vicinity of the glass-liquid transition at well-defined temperatures from a resistive state into a superconducting state ($R \equiv V/I = 0$, in the low current density limit) upon cooling, in an applied magnetic field lower than B_ϕ along the c axis. For a fixed filling fraction f_ϕ (i.e., $f \equiv \mu_0 H/B_\phi$), the typical isothermal I-V curves measured for BSCCO (sample 1) at $\mu_0 H = 0.25\ T$ are displayed in Fig. 1 on a log-log scale. As shown, the characteristics progressively shift from a linear response ($V \propto I$) for low current densities (solid lines) above T_{BG} to a power law regime at $T_{\mathrm{BG}}(V \propto I^\zeta)$ and finally to a strongly nonlinear response below the transition temperature ($V/I \propto \exp[-(I_0/I)^\mu]$). A similar set of $I(V)$ curves for KBBO is presented in Fig. 2. A very similar change in the curvature was observed in both systems. This result is expected for a glassy vortex system. Such typical behaviors can be explained based on the basis of the Bose-glass melting theory.[1] According to the predictions of Nelson and Vinokur for a Bose-glass transition in the presence of one-dimensional correlated disorder, the melting of the Bose glass can be described by a scaling formalism in which the correlation volume diverges at $T = T_{\mathrm{BG}}(\mu_0 H)$. This volume is anisotropic in the presence of columnar defects and the correlation lengths $\xi_\parallel$, parallel to, and $\xi_\perp$, perpendicular to, the columns obey the relation $\xi_\parallel \propto \xi_\perp^\alpha$ with $\alpha = 2$ in the case of screened vortex interactions ($\alpha = 1$ for isotropic pinning i.e. point disorder as well as for an incompressible Bose glass with long-range interactions).[15] In this model, dynamical predictions for transport measurements with the current density J applied perpendicular to CDs and the magnetic field **H** aligned with the correlated defects can be derived by a scaling ansatz as follows:

$$\frac{E}{J\xi_\parallel \xi_\perp^{-z}} = F_\pm\left(\frac{J\xi_\parallel \xi_\perp \phi_0}{K_B T}\right), \tag{1}$$

where $\xi_\perp(T) = \xi_\perp(0)|(T - T_{\mathrm{BG}})/T_{\mathrm{BG}}|^{-\nu_\perp}$, z is the critical exponent for the correlation time $\tau \propto \xi_\perp^z$ and F_+ and F_- are two scaling functions defined in the flux liquid state ($T > T_{\mathrm{BG}}$) and localized flux-line state ($T < T_{\mathrm{BG}}$), respectively. The scaling function $F_+(x) = \mathrm{const}$, $F-(x) \propto \exp(-1/x^\mu)$ for $x \to 0$ and $F_\pm(x \to \infty) \propto x^{(z+1)/(1+\alpha)}$. $\nu_\perp$ is the critical exponent describing the divergence of the correlation lengths $\xi_\parallel$ and $\xi_\perp$. Note that we set $\alpha(\equiv \nu_\parallel/\nu_\perp) = 2$ in order that the compressional modulus of the vortex-liquid phase $c_{11} \sim [K_B T(\mu_0 H)^2/\phi_0^2]/\xi_\perp^2 \xi_\parallel$ remains finite at $T = T_{\mathrm{BG}}$.[1] Thus, the only free parameters are z, $\nu_\perp$, and T_{BG}. In general, the

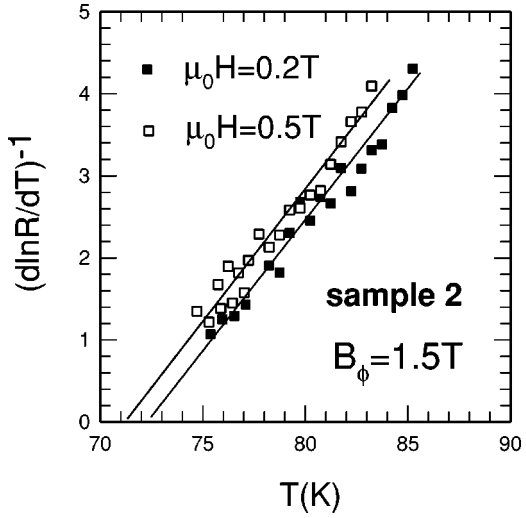

FIG. 3. Typical inverse of the logarithmic derivative of the resistance $R(T)$ for $\mu_0 H=0.2$ and 0.5 T. The solid lines represent the power law of $R=R_0(T-T_{\rm BG})^{\nu_\perp(z-2)}$, with a slope $[\nu_\perp(z-2)]^{-1}\sim 0.33$ and intercepts $T_{\rm BG}=72.4$ and 71 K, respectively.

estimated values of the dynamic exponent z and the static exponent $\nu_\perp$ are derived from a power law dependence $V\sim I^{(z+1)/(1+\alpha)}$ at $T=T_{\rm BG}$ (the slope of the dashed line $\zeta=(z+1)/(1+\alpha)$ in Fig. 1; $\zeta\sim 2$) and the fitting the ohmic resistance (linear part of *I-V* curves in the limit $I\to 0$) near $T_{\rm BG}$ in the thermally assisted flux-flow regime which should vanish according to $R\sim[(T-T_{\rm BG})/T_{\rm BG}]^{\nu_\perp(z-2)}$. In this basis, in the critical behavior where R follows the above power law, a plot of $(d\ln R/dT)^{-1}=(T-T_{\rm BG})/[\nu_\perp(z-2)]$ versus temperature should be a straight line with a slope equal to $1/[\nu_\perp(z-2)]$ intercepting the temperature axis at $T_{\rm BG}$. As shown in Fig. 3, the plot of $(d\ln R/dT)^{-1}=(T-T_{\rm BG})/[\nu_\perp(z-2)]$ versus temperature is consistent with this type of behavior. We obtained $[\nu_\perp(z-2)]\sim 3$ and $T_{\rm BG}=72.4$ and 71 K, for $\mu_0 H=0.2$ and 0.5 T. Combining these two measurements, we obtained $\nu_\perp\sim 1$ and $z\sim 5$. We also checked the *I-V* curves in the critical region scale, according to the Eq. (1), into two curves corresponding to F_+ and F_- with the obtained exponents. It can be seen clearly in the inset of Fig. 1 that all of the *I-V* isothermal characteristics around $T_{\rm BG}$ for sample 1 (BSCCO crystal) at different filling fractions $f=0.133$, 0.266, 0.4, 0.533, 0.666, and 0.8 collapse nicely onto two positive ($T>T_{\rm BG}$) and negative ($T<T_{\rm BG}$) curvature curves. From the scaling analysis, the optimum values of the critical exponents $z=5.3\pm 0.2$, $\nu_\perp=1.1\pm 0.1$, and $n=\nu_\perp(z-2)=3.63\pm 0.3$. Similar scaling behavior was achieved at $\mu_0 H=7T\sim B_\phi$ for sample 5 irradiated (KBBO crystal, $B_\phi=6$ T). Indeed, as shown in the inset of Fig. 2, all of the isothermal *I-V* curves collapse by plotting $R_{\rm scal}=(V/I)/|t|^{\nu_\perp(z-2)}$ against $I_{\rm scal}=I/(T|t|^{3\nu_\perp})$ using the data of Fig. 2. The vertical dashed line (see, for example, the inset of Fig. 1) gives an estimate for the current crossover separating the ohmic and non-ohmic behavior J^* which can be used to evaluate the correlation length. We got $(\xi_\parallel\xi_\perp)^{1/2}\sim 20-30$ Å at low temperature in all samples. The values of the critical exponents are similar to those obtained for samples 2, 3, and 4.

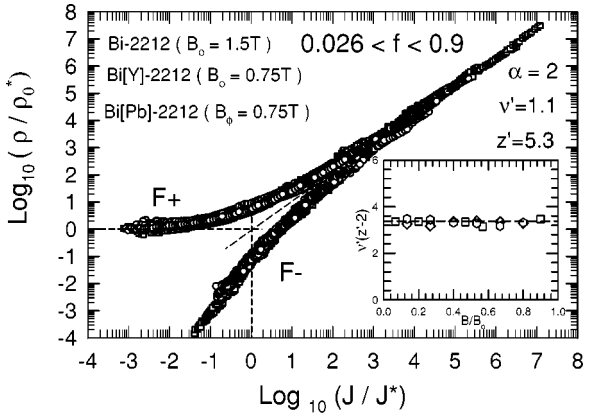

FIG. 4. Universal scaling forms for the resistivity obtained in all BSCCO samples over a wide range of filling factors $0.026\leqslant f\leqslant 0.9$. The scaling 4 is normalized by ρ_0^* and J^*. J^* is the current crossover separating the ohmic and non-ohmic regimes above $T_{\rm BG}$. The inset shows the filling factor independent combined critical exponents $n=\nu_\perp(z-2)$.

Our critical exponents are in a very good agreement with the numerical simulations for the case of the strongly screened vortex interactions.[15] Those exponents are also in a reasonable accord with those previously obtained in $Tl_2Ba_2CaCu_2O_8$ thin films.[16] However, in BSCCO, a combined critical exponents value $n=\nu_\perp(z-2)\sim 9$ and 8.5 has been extracted from the in-plane and out-of-plane resistivity data, respectively.[4,5] This value is surprisingly about three times larger than the one found in the present study. In YBCO, there is a large scattering in reported exponents values $\nu_\perp\sim 0.9-1.6$ and $z\sim 2.2-8.8$ in either single crystals or thin films.[3,6,17,18] The finding of critical exponents as $\nu_\perp\sim 1$, $z=2.2$, and $\alpha(\equiv\nu_\parallel/\nu_\perp)\sim 1$, by Jiang *et al.*[6] for an irradiated high quality single crystal, suggested that the Bose interaction is long ranged and the Bose-glass is incompressible.

The result in Fig. 4, whose axes are normalized when the resistivity is measured in units of $\rho_0^*(\rho_0^*\sim\rho_n)$ and the current in units of J^* ($J^*=J_0^*|t|^{\nu_\perp(1+\alpha)}$ with $J_0^*=K_BT/(\ell_{0\parallel}\ell_{0\perp})$), shows that the whole set of curves for the three different BSCCO samples and various magnetic fields ($B_\phi/10<\mu_0 H<B_\phi$) can be superimposed into two mains curves. We would emphasize two remarkable points. First, z and $\nu_\perp$ are found for all BSCCO samples to be insensitive to **H** over a range of fields corresponding to a filling fraction $0.133<f<0.9$ as shown in the inset of Fig. 4. Another important point is that the values of the critical exponents appear to be, within the experimental errors, sample and dose irradiation independent. Finally, our main result is the scaling collapse of the *I-V* curves for all samples. As shown in Fig. 5, the same scaling functions with the critical exponents $z=5.3\pm 0.2$ and $\nu_\perp=1.1\pm 0.1$ can be used for both BSCCO (samples 1, 2, and 3) and KBBO (samples 4 and 5) systems emphasizing the universality of the transition in this field range. Finally, note that we could not scale *I-V* curves for $\mu_0 H\leqslant B_\phi/10$ in either BSCCO or KBBO. We observed a very strong curvature that rapidly deviates from the high

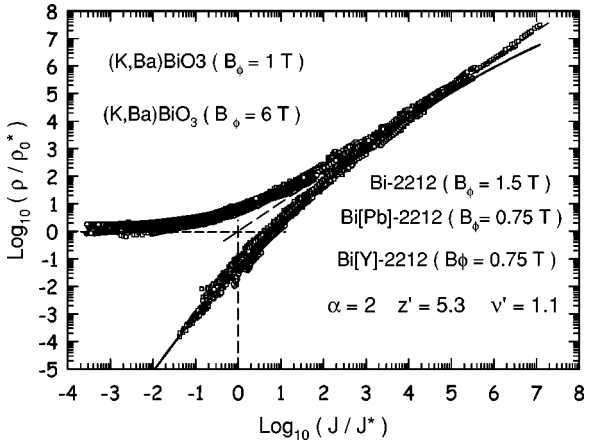

FIG. 5. Rescaled I-V characteristics using Eq. (1) (see the text for details) for all BSCCO and (K,Ba)BiO_3 samples. The solid line corresponds to a variable range hopping creep mechanism.

temperature linear regime, thus suggesting a much abrupt depinning of the vortices in this low field range.

B. Creep mechanism

We now investigate the Bose-glass phase itself ($T < T_{BG}$). In the Bose-glass phase, the vortex dynamics is determined by the current-dependent pinning barriers, which give a rise to a highly non-linear thermally activated regime[1,19]

$$E(J) = \rho_0 J \exp[-E_K/K_B T(J_c/J)^{\mu}], \tag{2}$$

where ρ_0 denotes the normal-state resistivity, E_K is the typical kink energy, and J_c is the characteristic current scale of the creep process. The value of the glassy exponent μ is regime specific and characterizes the creep process. With decreasing current, $\mu = 1$ and 1/3 for half loop and double-superkink excitations, respectively. In the limit of weak current densities and close to the transition, the most important mechanism for vortex transport is the tunneling between different columnar defects via the formation of a pair of ''superkinks'' in the analogy with the VRH transport of charge carriers between localized states in disordered semiconductors. In this case, the creep exponent is expected to be $\mu = 1/3$ for a noninteracting vortex (i.e., when the London penetration depth is considerably smaller than the average defect spacing $\lambda/d \ll 1$).[1] Taking the vortex-vortex interactions into account, by using numerical simulations, Täuber and Nelson, showed that these interactions led to the emergence of a Coulomb gap in the distribution of pinning energies, with the result that the glassy exponent μ varied in the range between 1/3 and 1.[20] For example, they found that for fillings $0.1 \leqslant f \leqslant 0.4$ and large value $\lambda/d \geqslant 5$ the creep exponent reached a maximum value of $\mu \approx 2/3$. Experimentally, the creep exponent was determined by calculating the logarithmic derivative of Eq. (2) with respect to J. We extracted the value of the glassy exponent μ by recasting Eq. (2) into the form $d[\ln(E/J)]/dJ = (\mu E_K/J_0 K_B T)(J_0/J)^{\mu+1}$ so that a log-log plot of the graph of $d[\ln(E/J)]/dJ$ versus J is a straight line, whose slope is equal to $-(\mu+1)$. Figure 6 displays log-log

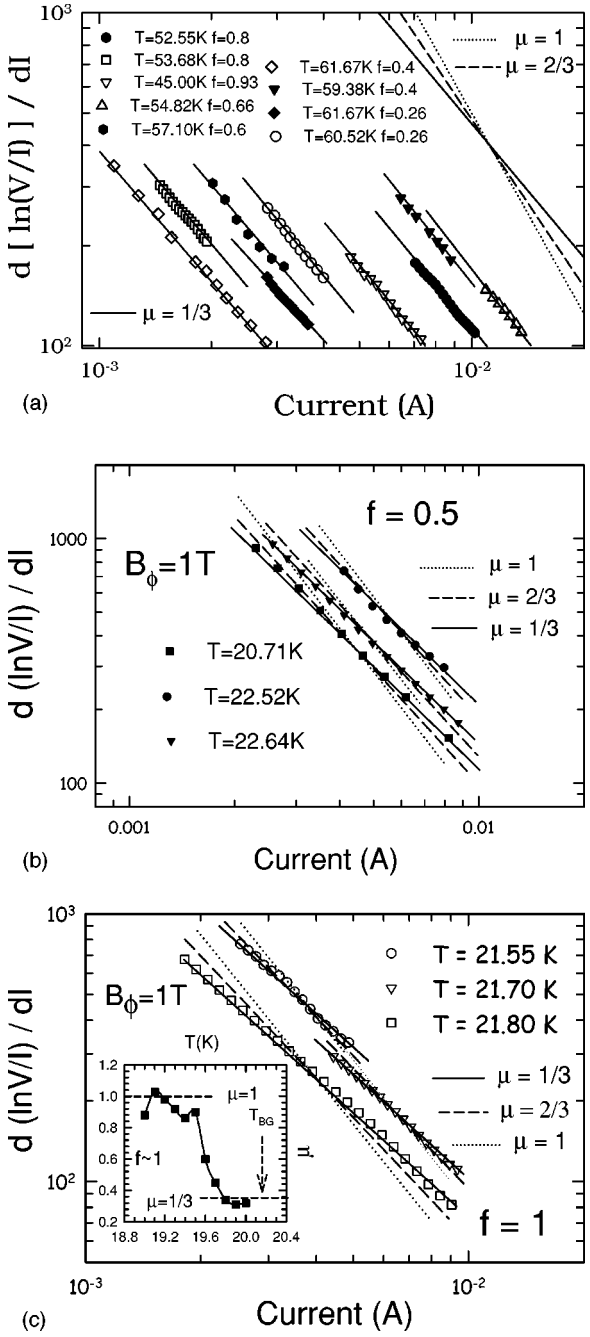

FIG. 6. A log-log plot of $d[\ln(V/I)]/dI$ vs I for **H** and T fixed in the Bose glass phase obtained (a) on sample 1 (Bi-2212 crystal: $B_\phi = 0.75$ T) and (b) and (c) sample 4 (KBBO crystal: $B_\phi = 1$ T). Inset of (c) the temperature dependence of the creep exponents for the KBBO sample 5 with $B_\phi = 6$ T and $\mu_0 H = 7$ T. The straight lines are regression lines from where we obtain the glassy exponent $\mu \sim 1/3$, which indicates that this creep proceeds via variable-range vortex hopping. In comparison, the dashed lines represent an attempt to fit $d[\ln(V/I)]/dI \sim (I)^{-(\mu+1)}$ with $\mu = 2/3$ and $\mu = 1$ which are typical for double-kink and half loop transport processes for flux lines, respectively.

plots of $d[\ln(V/I)]/dI$ versus I corresponding to typical isothermal I-V curves for BSCCO [Fig. 6(a)] and KBBO [Figs. 6(b) and 6(c)]. Parallel straight lines support Eq. (2) with a magnetic field independent exponent value $\mu \approx 1/3$, which is

in a good agreement with the VRH mechanism. In comparison, the dashed lines represent an attempt to fit $d[\ln(V/I)]/dI \sim (I)^{-(\mu+1)}$ with $\mu=2/3$ and $\mu=1$ which are typical of double-kink and half loop transport processes for flux lines, respectively. The glass exponent value $\mu \approx 1/3$ has been found over a wide filling range from 0.04 to 0.9 for long-range interactions ($\lambda/d \sim 10$) in both systems. This suggests that no Coulomb-gap-like feature occurs in the distribution of pinning energies. An extensive study of the vortex creep in BSCCO is presented in Ref. 21 and led to the same creep exponent. Thus the VRH seems to be the dominant mechanism for the vortex creep close to the transition and, as shown in Fig. 5 (solid line), $F-(x)$ is thus of the form $F-(x) \sim \exp[-(x_0/x)^{1/3}]$ in the low current limit. A similar creep process has been observed when **H** is tilted at an angle θ away from the column direction. Below the transition, the $I(V)$ curves can still be well fitted by the VRH up to $\theta \sim 25°$ and 20° in KBBO and BSCCO samples, respectively. For lower temperatures (that is for higher current densities), depinning occurs through the vortex half-loop activation mechanism characterized by a glassy exponent $\mu=1$ in BSCCO and KBBO systems.[22,23] The half-loop exponent $\mu=1$ has also been obtained from the frequency dependence of the ac transmittivity measurements on BSCCO crystals.[24,25] These experimental results obtained in both systems with very different electronic anisotropy and irradiation doses, universal scaling of *I-V* characteristics and flux-creep mechanism in the glassy state, were found to be consistent with the Bose glass predictions for vortex line pinning by columnar defects. The fact that the Bose-glass behavior is observed in highly anisotropic BSCCO with CDs indicates that the pancake vortices pinned by columnar tracks in heavy-ion irradiated BSCCO crystals behave as well-coupled vortex lines. The three-dimensional coupling of vortices by CDs was demonstrated by the transport measurements in flux transformer geometry[26] and Josephson plasma resonance in BSCCO with CDs.[27]

The main finding in this work is the evidence of strong similarities in the transport data obtained in KBBO and BSCCO single crystals with columnar defects. However, recent specific heat measurements in heavy irradiated KBBO crystals showed that the thermodynamic transition line deduced from specific heat measurements is directly related to the melting of the Bose glass.[28,29] Those experiments thus suggested that the scaling functions in KBBO seem to describe the transition between the superconducting and the normal states than the melting of the Bose glass in the so-called vortex liquid.[29] The observation of a universal scaling behavior in KBBO and BSCCO systems suggested that similar effects might be observed in irradiated high-T_c cuprates. Therefore, specific heat measurements on irradiated cuprates will be very helpful in order to clarify the origin of the scaling properties obtained by transport measurements.

IV. SUMMARY

I-V characteristics over a wide range of filling fraction $f=(\mu_0 H/B_\phi)$ were used to investigated vortex dynamics in heavily irradiated $Bi_2Sr_2CaCu_2O_{8+\delta}$ and $(K,Ba)BiO_3$ single crystals. We found a strong similarity between the Bose glass transitions in the highly anisotropic $Bi_2Sr_2CaCu_2O_{8+\delta}$ and the isotropic $(K,Ba)BiO_3$ systems. In both cases, the *I-V* characteristics could be described by the scaling laws predicted for the Bose-glass melting with $z=5.3\pm0.2$, $\nu_\perp=1.1\pm0.1$, and $\alpha(\equiv \nu_\parallel/\nu_\perp)=2$. These values were found reasonably consistent with those predicted to the Bose-glass-to-liquid from numerical simulations in the case of strongly screened vortex interactions. A detailed quantitative analysis of *I-V* curves in the glassy state indicated that the creep proceeds via variable-range hopping at low current close to T_{BG} and by half loop model at high current regime in both systems.

ACKNOWLEDGMENTS

We acknowledge enlightening discussions with T. Klein. We are grateful to J. Marcus for the preparation of the $(K,Ba)BiO_3$ single crystals. This work was supported by the CNRT-Région Centre (France).

*Corresponding author. Fax: +33 02 47 36 69 56; Email address: ammor@delphi.phys.univ-tours.fr

[1] D. R. Nelson and V. M. Vinokur, Phys. Rev. B **48**, 13060 (1993).
[2] L. Radzihovsky, Phys. Rev. Lett. **74**, 4923 (1995).
[3] R. J. Olsson, W. K. Kwok, L. M. Paulius, A. M. Petrean, D. J. Hofman, and G. W. Crabtree, Phys. Rev. B **65**, 104520 (2002).
[4] L. Mui, P. Wagner, A. Hadish, F. Hilmer, H. Adrian, J. Wiesner, and G. Wirth, Phys. Rev. B **51**, 3953 (1995).
[5] W. S. Seow, R. A. Doyle, A. M. Campbell, G. Balakrishnan, D. Mck. Paul, K. Kadowaki, and G. Wirth, Phys. Rev. B **53**, 14611 (1996).
[6] W. Jiang, N. C. Yeh, D. S. Reed, U. Kriplani, D. A. Beam, M. Konczykowski, T. A. Tombrello, and F. Holtzberg, Phys. Rev. Lett. **72**, 550 (1994).
[7] R. Sugano, T. Onogi, K. Hirata, and M. Tachiki, Phys. Rev. B **60**, 9734 (1999).
[8] A. Pomar, L. Martel, Z. Z. Li, and H. Raffy, Phys. Rev. B **63**, 134525 (2001).
[9] N. Kuroda, N. Ishikawa, Y. Chimi, A. Iwase, S. Okayasu, H. Ikeda, R. Yoshizaki, and T. Kambara, Physica C **321**, 143 (1999).
[10] T. Klein, A. Conde-Gallardo, J. Marcus, and C. Escribe-Filippini, Phys. Rev. B **58**, 12411 (1998); L. Baril, T. Klein, J. Marcus, and C. Escribe-Filippini, *ibid.* **54**, 16 058 (1996).
[11] I. Joumard, J. Marcus, T. Klein, and R. Cubitt, Phys. Rev. Lett. **82**, 4930 (1999).
[12] A. Ruyter, Ch. Simon, V. Hardy, M. Hervieu, and A. Maignan, Physica C **225**, 235 (1994).
[13] S. Hébert, V. Hardy, M. Hervieu, G. Villard, Ch. Simon, and J. Provost, Nucl. Instrum. Methods Phys. Res. B **146**, 545 (1998).
[14] T. Klein, A. Conde-Gallardo, I. Joumard, J. Marcus, C. J. van der Beek, and M. Konczykowski, Phys. Rev. B **61**, R3830 (2000).
[15] A. Vestergren, J. Lidmar, and M. Wallin, Phys. Rev. B **67**, 092501 (2003); J. Lidmar and M. Wallin, Europhys. Lett. **47**, 494 (1999); M. Wallin, E. S. Sorensen, S. M. Girvin, and A. P. Young, Phys. Rev. B **49**, 12115 (1994).

[16] V. Ta Phuoc, A. Ruyter, L. Ammor, A. Wahl, and J. C. Soret, Phys. Rev. B **56**, 122 (1997).
[17] A. Mazilu, H. Saffar, M. P. Maley, J. Y. Coulter, L. N. Bulaevskii, and S. Foltyn, Phys. Rev. B **58**, R8909 (1998).
[18] P. L. Gammel, L. F. Schneemeyer, and D. J. Bishop, Phys. Rev. Lett. **66**, 953 (1991).
[19] For a review, see G. Blatter, V. B. Geshkebein, V. B. Larkin, and V. M. Vinokur, Rev. Mod. Phys. **66**, 1125 (1994).
[20] U. C. Täuber and D. R. Nelson, Phys. Rev. B **52**, 16106 (1995); U. C. Täuber, H. Dai, D. R. Nelson, and C. M. Lieber, Phys. Rev. Lett. **74**, 5132 (1995).
[21] J. C. Soret, L. Ammor, V. Ta Phuoc, R. De Sousa, A. Ruyter, A. Wahl, and G. Villard, Solid State Commun. **109**, 461 (1999).
[22] V. T. Phuoc, E. Olive, R. De Sousa, A. Ruyter, L. Ammor, and J. C. Soret, Phys. Rev. Lett. **88**, 187002 (2002).
[23] T. Klein, J. Marcus, S. Blanchard C. J. van der Beek, and M. Konczykowski (unpublished).
[24] C. J. Van der Beek, M. Konczykowski, V. M. Vinokur, G. W. Crabtree, T. W. Li, and P. H. Kes, Phys. Rev. Lett. **74**, 1214 (1995); Phys. Rev. B **51**, 15492 (1995).
[25] M. Konczykowski, N. Chikumoto, V. M. Vinokur, and M. V. Feigelman, Phys. Rev. B **51**, 3957 (1995).
[26] R. A. Doyle, W. S. Seow, Y. Yan, A. M. Campbell, T. Mochiku, K. Kadowaki, and G. Wirth, Phys. Rev. Lett. **77**, 1155 (1996).
[27] T. Hanaguri, Y. Tsuchiya, S. Sakamoto, A. Meada, and D. G. Steel, Phys. Rev. Lett. **78**, 3177 (1997).
[28] S. Blanchard, T. Klein, J. Marcus, I. Joumard, A. Sulpice, P. Szabo, P. Samuely, A. G. M. Janse, and C. Marcenat, Phys. Rev. Lett. **88**, 177201 (2002).
[29] C. Marcenat, S. Blanchard, J. Marcus, L. M. Paulius, C. J. van der Beek, M. Konczykowski, and T. Klein, Phys. Rev. Lett. **90**, 037004 (2003).